

A Statistical Dynamical Model to Predict Extreme Events and Anomalous Features in Shallow Water Waves with Abrupt Depth Change

Andrew J. Majda^{a,1}, M. N. J. Moore^b, and Di Qi^{a,1}

^aDepartment of Mathematics and Center for Atmosphere and Ocean Science, Courant Institute of Mathematical Sciences, New York University, New York, NY 10012; ^bDepartment of Mathematics and Geophysical Fluid Dynamics Institute, Florida State University, Tallahassee, FL

This manuscript was compiled on November 24, 2018

Understanding and predicting extreme events and their anomalous statistics in complex nonlinear systems is a grand challenge in climate, material, and neuroscience, as well as for engineering design. Recent controlled laboratory experiments in weakly turbulent shallow water with abrupt depth change (ADC) exhibit a remarkable transition from nearly Gaussian statistics in incoming wave trains before the ADC to outgoing waves trains after the ADC with extreme anomalous statistics with large positive skewness of the surface height. Here we develop a statistical dynamical model to explain and quantitatively predict the above anomalous statistical behavior as experimental control parameters are varied. The first step is to use incoming and outgoing truncated Korteweg-de Vries (TKdV) equations matched in time at the ADC. The TKdV equation is a Hamiltonian system which induces incoming and outgoing statistical Gibbs invariant measures which are statistically matched at the ADC. The statistical matching of the known nearly Gaussian incoming Gibbs state at the ADC completely determines the predicted anomalous outgoing Gibbs state, which can be calculated by a simple sampling algorithm, verified by direct numerical simulations, and successfully captures key features of the experiment. There is even an analytic formula for the anomalous outgoing skewness. The strategy here should be useful for predicting extreme anomalous statistical behavior in other dispersive media in different settings.

extreme anomalous event | statistical TKdV model | matching Gibbs measures | surface wave displacement and slope

Understanding and predicting extreme events and their anomalous statistics in complex nonlinear systems is a grand challenge in climate, material and neuroscience as well as for engineering design. This is a very active contemporary topic in applied mathematics with qualitative and quantitative models (?) and novel numerical algorithms which overcome the curse of dimension for extreme event prediction in large complex systems (?). The occurrence of Rogue waves as extreme events with different physical settings of deep water (?) and shallow water (?) is an important practical topic.

Recent controlled laboratory experiments in weakly turbulent shallow water with abrupt depth change (ADC) exhibit a remarkable transition from nearly Gaussian statistics in incoming wave trains before the ADC to outgoing waves trains after the ADC with extreme anomalous statistics with large positive skewness of the surface height (?). Here we develop a statistical dynamical model to explain and quantitatively predict the above anomalous statistical behavior as experimental control parameters are varied. The first step is to use incoming and outgoing truncated Korteweg-de Vries (TKdV) equations matched in time at the ADC. The TKdV equation is a Hamil-

tonian system which induces incoming and outgoing statistical Gibbs invariant measures which are statistically matched at the ADC. The statistical matching of the known nearly Gaussian incoming Gibbs state at the ADC completely determines the predicted anomalous outgoing Gibbs state, which can be calculated by a simple MCMC algorithm, verified by direct numerical simulations, and successfully captures key features of the experiment. There is even an analytic formula for the anomalous outgoing skewness. The strategy here should be useful for predicting extreme anomalous statistical behavior in other dispersive media in different settings.

1. Experiments showing anomalous wave statistics by the abrupt depth change

A series of experiments are carried out (?) studying the anomalous statistical behaviors in surface water waves going through an abrupt depth transition. The unidirectional waves propagate along a water tank over a step in the bottom topography, and the surface displacements of the wave levels are measured at several upstream and downstream locations. The

Significance Statement

Understanding and predicting extreme events and their anomalous statistics in complex nonlinear systems is a grand challenge in applied sciences as well as for engineering design. Recent controlled laboratory experiments in weakly turbulent shallow water with abrupt depth change exhibit a remarkable transition from nearly Gaussian statistics to extreme anomalous statistics with large positive skewness of the surface height. We develop a statistical dynamical model to explain and quantitatively predict the anomalous statistical behavior. The incoming and outgoing waves are modeled by the truncated Korteweg-de Vries equations statistically matched at the depth change. The statistical matching of the known nearly Gaussian incoming Gibbs state completely determines the predicted anomalous outgoing Gibbs state, and successfully captures key features of the experiment.

A.J.M. designed the research. A.J.M., M.N.J.M., and D.Q. performed the research. A.J.M., M.N.J.M., and D.Q. wrote the paper.

The authors declare no conflict of interest.

¹To whom correspondence should be addressed. E-mail: qidi@cims.nyu.edu, jon-jon@cims.nyu.edu

wave field is excited by a paddle wheel forcing with angle

$$\theta(t) = \theta_0 + \Delta\theta \sum_{n=1}^N a_n \cos(\omega_n t + \delta_n), E \sim (\Delta\theta)^2 \sum_n a_n^2 \omega_n^2.$$

The total energy E in the system is determined by the angle amplitude $\Delta\theta$. Several observations are found in the anomalous wave statistics:

- Distinct statistics are found between the incoming and outgoing wave disturbances: the incoming waves display near-Gaussian statistics, while the outgoing waves show skewness toward the positive displacement.
- The non-Gaussian statistics is related with the total energy contained in the system: larger driving amplitude $\Delta\theta$ will generate stronger skewness in the PDFs.
- The waves also show different characteristic peak wavelengths in incoming and outgoing flows.

2. Surface wave turbulence modeled by truncated KdV equation with depth dependence

The surface wave turbulence is modeled by a one-dimensional deterministic dynamical model. The Korteweg-de Vries (KdV) equation (?) is a leading-order approximation of the surface waves that are determined by the balance of nonlinear and dispersive effects in an appropriate far-field limit. Here, the KdV equation is truncated in the first Λ modes (with $J = 2\Lambda + 1$ grid points) to generate weakly turbulent dynamics. Therefore, the surface disturbance is modeled by the state variable $u_\Lambda^\pm(x, t)$ with superscript ‘-’ for the incoming waves and ‘+’ for the outgoing waves. The Galerkin truncated variable $u_\Lambda = \sum_{1 \leq |k| \leq \Lambda} \hat{u}_k(t) e^{ikx}$ is normalized with zero mean $\hat{u}_0 = 0$ and unit energy $2\pi \sum_{k=1}^\Lambda |\hat{u}_k|^2 = 1$, which are conserved quantities, and $u_\Lambda \equiv \mathcal{P}_\Lambda u$ denotes the subspace projection. The motion is governed by the truncated KdV equation with depth change D_\pm about the state variable u_Λ^\pm

$$\frac{\partial u_\Lambda^\pm}{\partial t} + \frac{D_\pm^{-3/2}}{2} E_0^{1/2} L_0^{-3/2} \frac{\partial}{\partial x} \mathcal{P}_\Lambda (u_\Lambda^\pm)^2 + D_\pm^{1/2} L_0^{-3} \frac{\partial^3 u_\Lambda^\pm}{\partial x^3} = 0, \quad [1]$$

on the normalized periodic domain $x \in [-\pi, \pi]$ with the conserved Hamiltonian decomposed into the difference of two components containing the cubic and quadratic terms

$$\begin{aligned} \mathcal{H}_\Lambda^\pm &= D_\pm^{-3/2} E_0^{1/2} L_0^{-3/2} H_3(u_\Lambda^\pm) - D_\pm^{1/2} L_0^{-3} H_2(u_\Lambda^\pm), \\ H_3(u) &= \frac{1}{6} \int_{-\pi}^{\pi} u^3 dx, \quad H_2(u) = \frac{1}{2} \int_{-\pi}^{\pi} \left(\frac{\partial u}{\partial x} \right)^2 dx. \end{aligned}$$

The model [??] is non-dimensionalized in the periodic domain. The depth is assumed to be unit $D_- = 1$ before the abrupt depth change and becomes $D_+ < 1$ for the flows after the change. We introduce the model parameters (E_0, L_0, Λ) based on the following model assumptions:

- The wavenumber truncation Λ is fixed in a moderate value for generating weakly turbulent dynamics;
- The state variable u_Λ^\pm is normalized with zero mean and unit energy, $\mathcal{M}(u_\Lambda) = 0, \mathcal{E}(u_\Lambda) = 1$, conserved during the evolution, while E_0 characterizes the total energy injected in the system based on the paddle amplitude $(\Delta\theta)^2$;

125

126

127

- The length scale of the system is defined by L_0 . The value is chosen so that the resolved scale $\Delta x = 2\pi L_0/J$ is comparable with the the characteristic wave length λ_c found from the experiments.

132

The intention for the distinct model dynamics comes from the balance between the cubic and quadratic terms in the Hamiltonian \mathcal{H}_Λ^\pm . After the depth change, $D_+ < 1$, more weight is added to the cubic term, H_3 , for stronger nonlinearity and weaker dispersion for the third-order derivative term reflected by the smaller coefficient for H_2 in the Hamiltonian. Since $\frac{\partial u}{\partial x}$ is the slope of the wave height, $H_2(u)$ measures the wave slope energy.

A *deterministic matching condition* is given for the surface displacement u_Λ^\pm agreeing at the locations before and after the abrupt depth change T_{ADC}

144

$$145 \quad u_\Lambda^-(x, t) |_{t=T_{ADC}-} = u_\Lambda^+(x, t) |_{t=T_{ADC}+},$$

146

assuming the abrupt depth change is met at $t = T_{ADC}$. Equation [??] is not designed to capture the short scale changes in rapid time. On the other hand, we are interested in the model statistic transition before and after the depth change, so it is reasonable to observe the suitable slow-time performance in the large-scale structures.

153

Interpreting experimental parameters in the dynamical model.

The model parameters (E_0, L_0, Λ) in [??] can be directly linked with the basic scales from the physical problem. The important characterizing parameters measured from the experiments include $\epsilon = \frac{a}{H_0}$ the wave amplitude a to water depth H_0 ratio; $\frac{H_0}{\lambda_c}$ the water depth to wavelength scale λ_c ratio; and $D_0^{1/2} \frac{d}{H_0}$ the normalized wave depth ratio with incoming flow depth $d = H_0$ to the outgoing flow depth $d < H_0$. The interpretations and reference values of these model parameters are based on the experimental setup (?). By comparing the characteristic physical scales, the normalized TKdV equation [??] can be linked directly with the measured non-dimensional quantities by

167

$$168 \quad 169 = 6^{\frac{1}{3}} \left(M \epsilon^{\frac{1}{2}} \delta^{-1} \right), \quad E_0 = \frac{27}{2} \gamma^{-2} \left(M \epsilon^{\frac{1}{2}} \delta^{-1} \right), \quad [2]$$

170

where M defines the computational domain size $L_d = M \lambda_c$ as M -multiple of the characteristic wavelength λ_c , and $\gamma = \frac{U}{a}$ represents the factor to normalize the total energy in the state variable u_Λ to one.

Consider the spatial discretization $J = 2\Lambda + 1$ so that the smallest resolved scale is comparable with the characteristic wavelength

178

$$179 \quad 180 \quad \frac{2\pi M \lambda_c}{J} \lesssim \lambda_c \Rightarrow M = \frac{J}{2\pi} \sim 5, \quad J = 32.$$

Therefore in the practical numerical simulations, we pick $M = 5$ and γ varies in the range $[0.5, 1]$. Using the reference experimental measurements (?), $\epsilon \in [0.0024, 0.024]$, $\delta \sim 0.22$, and $D_0^{1/2}$ changes from 1 to 0.24 before and after the depth change. The reference values for the model scales can be estimated in the range $L_0 \in [2, 6]$ and $E_0 \in [50, 200]$. These are the values we will test in the direct numerical simulations. See details about the derivation from scale analysis in *SI Appendix, A*.

3. Equilibrium statistical mechanism for generating the stationary invariant measure

Since the TKdV equation satisfies the Liouville property, the equilibrium invariant measure can be described by an equilibrium statistical formulism (??) using a Gibbs measure with the conserved energy \mathcal{E}_Λ and Hamiltonian \mathcal{H}_Λ . The equilibrium invariant measure is dictated by the conservation laws in the TKdV equation. In the case with fixed total energy E_0 , this is the *mixed Gibbs measure* in the truncated model with microcanonical energy and canonical Hamiltonian ensembles (??)

$$\mathcal{G}_\theta^\pm(u_\Lambda^\pm; E_0) = C_\theta^\pm \exp(-\theta^\pm \mathcal{H}(u_\Lambda^\pm)) \delta(\mathcal{E}(u_\Lambda^\pm) - E_0), \quad [3]$$

with θ representing the “inverse temperature”. The distinct statistics in the upstream and downstream waves can be controlled by the parameter value of the inverse temperature. The negative temperature regime, $\theta^\pm < 0$, is the appropriate regime to predict the experiments as shown below. In the incoming flow field, the inverse temperature θ^- is chosen so that \mathcal{G}_θ^- has Gaussian statistics. Using the above invariant measures [??], the expectation of any functional $F(u)$ can be computed based on the Gibbs measure

$$\langle F \rangle_{\mathcal{G}_\theta} \equiv \int F(u) \mathcal{G}_\theta(u) du.$$

The value of θ in the invariant measure is specified from $\langle H_\Lambda \rangle_{\mathcal{G}_\theta}$ (??). The invariant measure also predicts an equilibrium energy spectrum without running the TKdV equation directly. On the other hand, the time autocorrelation and transient statistics about the state variable u_Λ cannot be recovered from the statistical theory.

Statistical matching condition in invariant measures before and after the abrupt depth change. The Gibbs measures \mathcal{G}_θ^\pm are defined based on the different inverse temperatures θ^\pm on the two sides of the solutions

$$\begin{aligned} \mu_t^-(u_\Lambda^-; D_-), \quad u_\Lambda |_{t=T_{ADC}-} &= u_0, \quad t < T_{ADC}; \\ \mu_t^+(u_\Lambda^+; D_+), \quad u_\Lambda |_{t=T_{ADC}+} &= u_0, \quad t > T_{ADC}, \end{aligned}$$

where u_0 represents the deterministic matching condition between the incoming and outgoing waves. The two distributions, μ_t^-, μ_t^+ should also be matched at the depth change location T_{ADC} , so that

$$\mu_\infty^-(u_\Lambda) = \mu_{t=T_{ADC}}^-(u_\Lambda) = \mu_{t=T_{ADC}}^+(u_\Lambda).$$

In matching the flow statistics before and after the abrupt depth change, first we use the conservation of the deterministic Hamiltonian H_Λ^+ after the depth change. Then assuming ergodicity (??), the statistical expectation for the Hamiltonian $\langle H_\Lambda^+ \rangle$ is conserved in time after the depth change at $t = T_{ADC}$ and should stay in the same value as the system approaches equilibrium as $t \rightarrow \infty$. The final statistical matching condition to get the outgoing flow statistics with parameter θ^+ can be found by

$$\langle H_\Lambda^+ \rangle_{\mathcal{G}_\theta^+} = \langle H_\Lambda^+ \rangle_{\mathcal{G}_\theta^-}, \quad [4]$$

with the outgoing flow Hamiltonian H_Λ^+ and the Gibbs measures \mathcal{G}_θ^\pm before and after the abrupt depth change.

249

250

251

4. The nearly Gaussian incoming statistical state

252

253 The incoming flow is always characterized by a near-Gaussian distribution in the wave displacement. It is found that a physically 254 consistent Gibbs measure should take negative values in the 255 inverse temperature parameter $\theta < 0$, where a proper 256 distribution function and a decaying energy spectrum are 257 generated (see (??) and *SI Appendix, B.1* for the explicit 258 simulation results). The upstream Gibbs measure \mathcal{G}_θ^- with 259 $D_- = 0.24$ displays a wide parameter regime in (θ^-, E_0) with 260 near-Gaussian statistics. In the left panel of Figure ?? (a), the 261 inflow skewness κ_3^- varies only within small amplitudes among 262 changing values of E_0 and θ^- . The incoming flow PDF then 263 can be determined by picking the proper parameter value θ^- 264 in the near Gaussian regime with small skewness. In contrast, 265 the downstream Gibbs measure \mathcal{G}_θ^+ with $D_+ = 0.24$ shown in 266 the right panel of Figure ?? (a) generates much larger skewness 267 κ_3^+ with highly skewed PDFs as the absolute value of θ^+ and 268 the total energy level E_0 increase in amplitude. The solid lines 269 in Figure ?? (c) offer a further confirmation of the transition 270 from near-Gaussian statistics with tiny κ_3^- to strongly skewed 271 distribution κ_3^+ after the depth change.

272 In the next step, the value of the downstream θ^+ is determined 273 based on the matching condition [??]. The expectation 274 $\langle H_\Lambda^+ \rangle_{\mathcal{G}_\theta^+}$ about the incoming flow Gibbs measure can be calculated 275 according to the predetermined parameter values of 276 θ^- as well as E_0 from the previous step. For the direct 277 numerical experiments shown later in Figure ??, we pick proper 278 choices of test parameter values as $L_0 = 6, E_0 = 100$ and 279 $\theta^- = -0.3, -0.5$. More test cases with different system 280 energy 281 can be found in *SI Appendix, B.2* where similar 282 transitions from near Gaussian symmetric PDFs to skewed 283 PDFs in the flow state u_Λ^\pm can always be observed.

284

285 **Direct numerical model simulations.** Besides the prediction of 286 equilibrium statistical measures from the equilibrium statistical 287 approach, another way to predict the downstream model 288 statistics is through running the dynamical model [??] directly. 289 The TKdV equation is found to be ergodic with proper mixing 290 property as measured by the decay of autocorrelations as long 291 as the system starts from a negative inverse temperature state 292 as described before. For direct numerical simulations of the 293 TKdV equations, a proper symplectic integrator is required to 294 guarantee the Hamiltonian and energy are conserved in time. 295 It is crucial to use the symplectic scheme to guarantee the 296 exact 297 conservation of the energy and Hamiltonian since they 298 are playing the central role in generating the invariant measure 299 and the statistical matching. The symplectic schemes used 300 here for the time integration of the equation is the 4th-order 301 midpoint method (??). Details about the mixing properties 302 from different initial states and the numerical algorithm are 303 described in *SI Appendix, C*.

304

305

5. Predicting extreme anomalous behavior after the ADC by statistical matching

306

307 With the inflow statistics well described and the numerical 308 scheme set up, we are able to predict the downstream anomalous 309 statistics starting from the near-Gaussian incoming flow 310 going through the abrupt depth change from $D_- = 1$ to 311 $D_+ = 0.24$. First, we consider the statistical prediction in the 312 downstream equilibrium measure directly from the matching 313

376 as the flow goes through the abrupt depth change. The first
 377 row plots the changes in the skewness and kurtosis for the
 378 state variable u_Λ after the depth change at $t = 0$. The PDFs
 379 in the incoming and outgoing flow states are compared with
 380 three different initial inverse temperatures θ^- . After the depth
 381 changes to $D_0 = 0.24$ abruptly at $t = 0$, both the skewness
 382 and kurtosis jump to a much larger value in a short time,
 383 implying the rapid transition to a highly skewed non-Gaussian
 384 statistical regime after the depth change. Further from Figure
 385 ??, different initial skewness (but all relatively small) is set
 386 due to the various values of θ^- . With small $\theta^- = -0.1$, the
 387 change in the skewness is not very obvious (see the second
 388 row of Figure ?? for the incoming and outgoing PDFs of u_Λ).
 389 In comparison, if the incoming flow starts from the initial
 390 parameter $\theta^- = -0.3$ and $\theta^- = -0.5$, much larger increase
 391 in the skewness is induced from the abrupt depth change.
 392 Furthermore, in the detailed plots in the third row of Figure
 393 ?? for the downstream PDFs under logarithmic scale, fat tails
 394 towards the positive direction can be observed, which represent
 395 the extreme events in the downstream flow (see also Figure
 396 ?? for the time-series of u_Λ).
 397

398 As a result, the downstream statistics in final equilibrium
 399 predicted from the direct numerical simulations here agree with
 400 the equilibrium statistical mechanism prediction illustrated in
 401 Figure ???. The prediction from these two different approaches
 402 confirm each other.

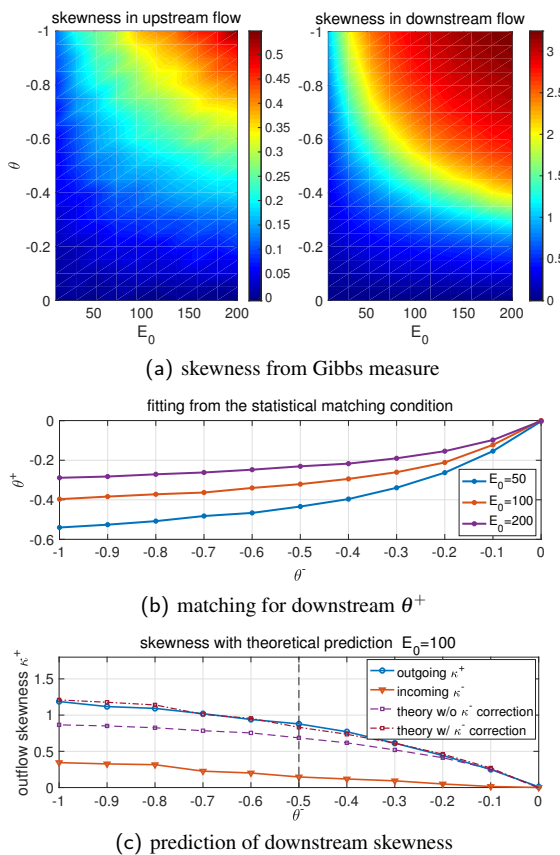


Fig. 1. First row: skewness from the Gibbs measures in incoming and outgoing flow states with different values of total energy E_0 and inverse temperature θ (notice the different scales in the incoming and outgoing flows); Second row: outgoing flow parameter θ^+ as a function of the incoming flow θ^- computed from the statistical matching condition with three energy level E_0 ; Last row: skewness in the outgoing flow with the matched value of θ^+ as a function of the inflow parameter θ^- (the theoretical predictions using [??] are compared).

condition. The downstream parameter value θ^+ is determined by solving the nonlinear equation [??] as a function of θ^+ , $F(\theta^+) = \langle H_\Lambda^+ \rangle_{\mathcal{G}_\theta^+}(\theta^+) - \langle H_\Lambda^+ \rangle_{\mathcal{G}_\theta^-} = 0$. In the numerical approach, we adopt a modified secant method avoiding the stiffness in the parameter regime (see the *SI Appendix, B.2* for the algorithm). The fitted solution is plotted in Figure ?? (b) as a function of the proposed inflow θ^- . A nonlinear $\theta^- - \theta^+$ relation is discovered from the matching condition. The downstream inverse temperature θ^+ will finally saturate at some level. The corresponding downstream skewness of the wave displacement u_Λ predicted from the statistical matching of Gibbs measures is plotted in Figure ?? (c). In general, a large positive skewness for outgoing flow κ_3^+ is predicted from the theory, while the incoming flow skewness κ_3^- is kept in a small value in a wide range of θ^- . Note that with $\theta^- \sim 0$ (that is, using the microcanonical ensemble only with energy conservation), the outflow statistics are also near Gaussian with weak skewness. The skewness in the outflow statistics grows as the inflow parameter value θ^- increases in amplitude.

For a second approach, we can use direct numerical simulations starting from the initial state sampled from the incoming flow Gibbs measure \mathcal{G}_θ^- and check the transient changes in the model statistics. Figure ?? illustrates the change of statistics

406 A statistical link between the upstream and downstream en-
 407 ergy spectra can be found for an analytical prediction of the
 408 skewness in the flow state u after the ADC. The skewness of
 409 the state variable u_j at one spatial grid point is defined as the
 410 ratio between the third and second moments

$$411 \quad 412 \quad \kappa_3 = \langle u_j^3 \rangle_\mu / \langle u_j^2 \rangle_\mu^{\frac{3}{2}}. \\ 413$$

414 Now we introduce mild assumptions on the distribution func-
 415 tions:

- 416 The upstream equilibrium measure μ_- has a relatively
 417 small skewness so that

$$418 \quad 419 \quad \langle H_3 \rangle_{\mu_-} = \frac{1}{6} \int_{-\pi}^{\pi} \langle u^3 \rangle_{\mu_-} dx \equiv \epsilon; \\ 420 \quad 421$$

- 422 The downstream equilibrium measure μ_+ is homogeneous
 423 at each physical grid point, so that the second and third
 424 moments are invariant at each grid point

$$425 \quad 426 \quad \langle u_j^2 \rangle_{\mu_+} = \sigma^2 = \pi^{-1}, \quad \langle u_j^3 \rangle_{\mu_+} = \sigma^3 \kappa_3 = \pi^{-\frac{3}{2}} \kappa_3^+. \\ 427$$

428 Then the skewness of the downstream state variable u_Λ^+ after
 429 the ADC is given by the difference between the inflow and
 430 outflow wave slope energy of u_x

$$431 \quad 432 \quad \kappa_3^+ = \frac{3}{2} \pi^{\frac{1}{2}} L_0^{-\frac{3}{2}} E_0^{-\frac{1}{2}} D_+^2 \int_{-\pi}^{\pi} \left[\langle u_x^2 \rangle_{\mu_+} - \langle u_x^2 \rangle_{\mu_-} \right] dx \\ 433 \quad 434 \quad + 3\pi^{\frac{1}{2}} \epsilon. \quad [5]$$

The detailed derivation is shown in *SI Appendix, B.2*. In particular, the downstream skewness with near-Gaussian inflow

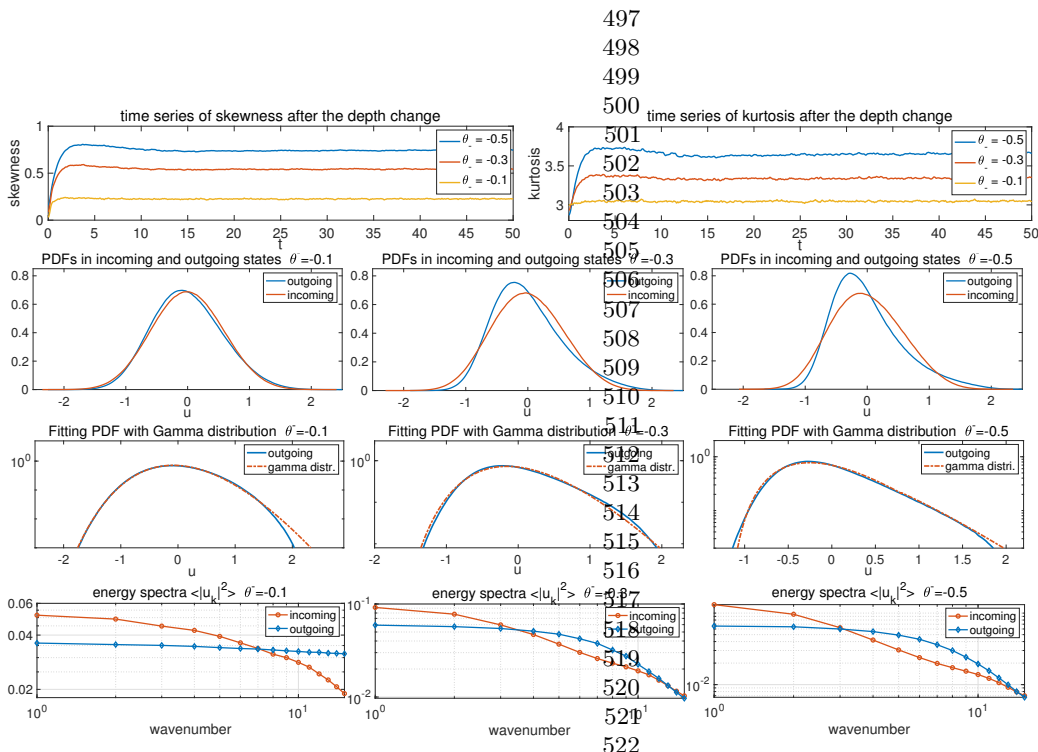


Fig. 2. Changes in the statistics of the flow state going through the abrupt depth change. The initial ensemble is set with the incoming flow Gibbs measure with different inverse temperature θ^- . First row: time evolution of the skewness and kurtosis. The abrupt depth change taking place at $t = 0$; Second row: inflow and outflow PDFs of u_Λ ; Third row: the downstream PDFs fitted with Gamma distributions with consistent variance and skewness (in log coordinate in y); Last row: energy spectra in the incoming and outgoing flows.

statistics $\epsilon \ll 1$ is positive if and only if the difference of the incoming and outgoing wave slope energy is positive. This means that there is more small scale wave slope energy in the outgoing state. As an evidence, in the last row of Figure ?? in all the weak and strong skewness cases, the outflow energy spectrum always has a slower decay rate than the inflow energy spectrum which possesses stronger energy in larger scales and weaker energy in the smaller scales.

In Figure ?? (c), we compare the accuracy of the theoretical estimation [??] with numerical tests. In the regime with small incoming inverse temperature θ^- , the theoretical formula offers a quite accurate approximation of the third-order skewness using only information from the second-order moments of the wave-slope spectrum.

7. Key features from experiments captured by the statistical dynamical model

In this final section, we emphasize the crucial features generated by the statistical dynamical model [??] by making comparison with the experimental observations in (?). As from the scale analysis displayed in Section ??, the theory is set in the same parameter regime as the experimental setup.

- The transition from near-Gaussian to skewed non-Gaussian distribution as well as the jump in both skewness and kurtosis observed in the experiment observations (Fig. 1 of (?)) can be characterized by the statistical model simulation results (see the first and second row of Figure ??). Notice that the difference in the decay of third and fourth moments in the far end of the downstream regime from the experimental data is due to the dissipation effect in the flow from the wave absorbers that is not modeled in the statistical model here. The model simulation

time-series plotted in Figure ?? can be compared with the observed time sequences from experiments (Fig. 1 of (?)). The downstream simulation generates waves with strong and frequent intermittency towards the positive displacement, while the upstream waves show symmetric displacements in two directions with at most small peaks in slow time. Even in the time-series at a single location $x=0$, the long-time variation displays similar structures.

- The downstream PDFs in experimental data are estimated with a Gamma distribution in Fig. 2 of (?). Here in the same way, we can fit the highly skewed outgoing PDFs from the numerical results with the Gamma distribution

$$\rho(u; k, \alpha) = \frac{e^{-k} \alpha^{-1}}{\Gamma(k)} (k + \alpha^{-1} u)^{k-1} e^{-\alpha^{-1} u}.$$

The parameters (k, α) in the Gamma distribution are fitted according to the measured statistics in skewness and variance, that is, $\sigma^2 = k\alpha^2$, $\kappa_3 = 2/\sqrt{k}$. And the excess kurtosis of the Gamma distribution can be recovered as $\kappa_4 = 6/k$. As shown in the third row of Figure ??, excellent agreement in the PDFs with the Gamma distributions is reached in consistency with the experimental data observations. The accuracy with this approximation increases as the initial inverse temperature θ^- increases in value to generate more skewed distribution functions.

- The experiments also have the up and down stream power spectra in time (Fig. 4 of (?)), which shows more energy at small time scales, i.e., a relatively slower decay rate in the downstream compared with the upstream case. This is also observed in the direct numerical simulations here (detailed results shown in *SI Appendix, C.2*). The

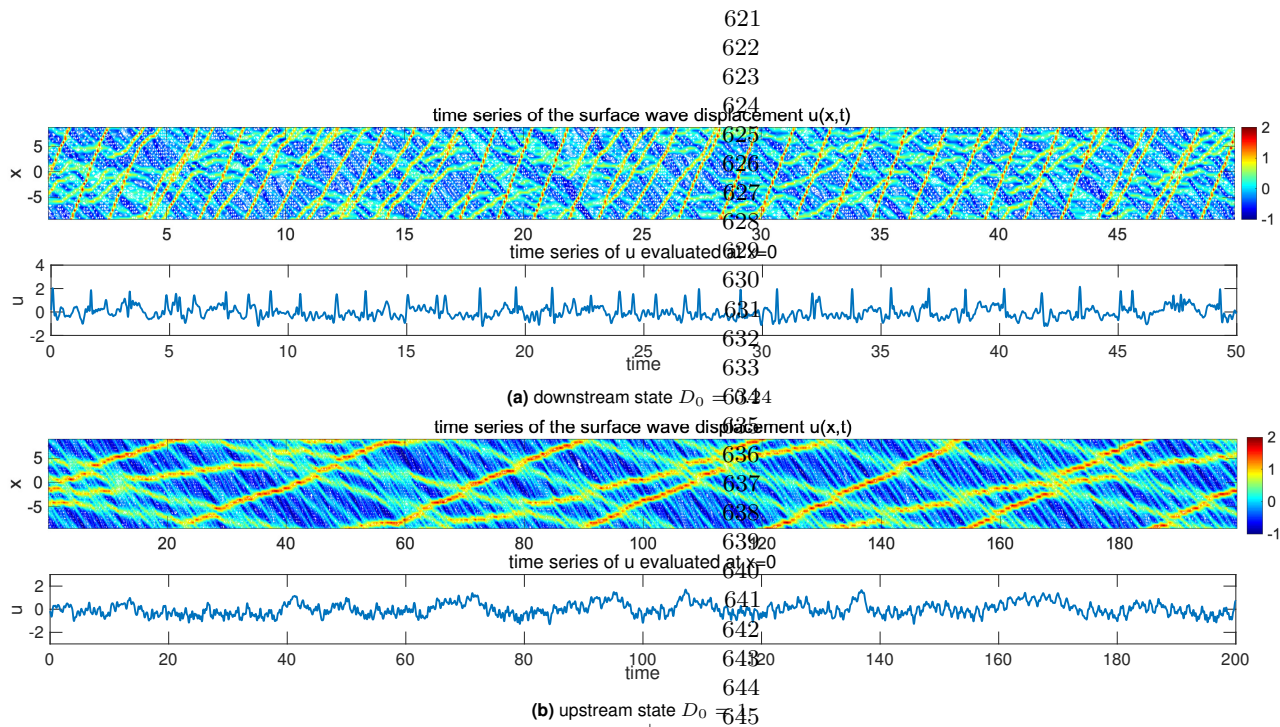


Fig. 3. Realization of the downstream and upstream flow solutions u_A^\pm . Note the larger vertical scale in the downstream time-series plot.

downstream state contains more energetic high frequencies. The peak frequency illustrates the occurrence of the transporting waves along the water tank.

8. Concluding discussion

We have developed a statistical dynamical model to explain and predict extreme events and anomalous features in shallow water waves with abrupt depth change. The theory is based on the dynamical modeling strategy consisting of the TKdV equation matched at the abrupt depth change with conservation of energy and Hamiltonian. Predictions can be made of the extreme events and anomalous features by matching incoming and outgoing statistical Gibbs measures before and after the abrupt depth transition. The statistical matching of the known

nearly Gaussian incoming Gibbs state completely determines the predicted anomalous outgoing Gibbs state, which can be calculated by a simple sampling algorithm, verified by direct numerical simulations, and successfully captures key features of the experiment. An analytic formula for the anomalous outgoing skewness is also derived. The strategy here should be useful for predicting extreme statistical events in other dispersive media in different settings.

ACKNOWLEDGMENTS. This research of A. J. M. is partially supported by the Office of Naval Research through MURI N00014-16-1-21619 D. Q. is supported as a postdoctoral fellow on the second grant. M.N.J.M would like to acknowledge support from Simons grant 524259.

1. Majda AJ, Branicki M (2012) Lessons in uncertainty quantification for turbulent dynamical systems. *Discrete & Continuous Dynamical Systems-A* 32(9):3133–3221.
2. Mohamad MA, Sapsis TP (2018) A sequential sampling strategy for extreme event statistics in nonlinear dynamical systems. *Proceedings of the National Academy of Sciences* 115(44):11138–11143.
3. Qi D, Majda AJ (2016) Predicting fat-tailed intermittent probability distributions in passive scalar turbulence with imperfect models through empirical information theory. *Communications in Mathematical Sciences* 14(6):1687–1722.
4. Majda AJ, Tong XT (2015) Intermittency in turbulent diffusion models with a mean gradient. *Nonlinearity* 28(11):4171–4208.
5. Majda AJ, Chen N (2018) Model error, information barriers, state estimation and prediction in complex multiscale systems. *Entropy* 20(9):644.
6. Majda AJ, Tong XT (2018) Simple nonlinear models with rigorous extreme events and heavy tails. *arXiv preprint arXiv:1805.05615*.
7. Thual S, Majda AJ, Chen N, Stechmann SN (2016) Simple stochastic model for el niño with westerly wind bursts. *Proceedings of the National Academy of Sciences* 113(37):10245–10250.
8. Chen N, Majda AJ (2018) Efficient statistically accurate algorithms for the Fokker–Planck equation in large dimensions. *Journal of Computational Physics* 354:242–268.
9. Chen N, Majda AJ (2017) Beating the curse of dimension with accurate statistics for the Fokker–Planck equation in complex turbulent systems. *Proceedings of the National Academy of Sciences* 114(49):12864–12869.
10. Chen N, Majda AJ (2018) Conditional Gaussian systems for multiscale nonlinear stochastic systems: Prediction, state estimation and uncertainty quantification. *Entropy* 20(7):509.
11. Qi D, Majda AJ (2018) Predicting extreme events for passive scalar turbulence in two-layer baroclinic flows through reduced-order stochastic models. *Communications in Mathematical Sciences* 16(1):17–51.
12. Adcock TA, Taylor PH (2014) The physics of anomalous ('rogue') ocean waves. *Reports on Progress in Physics* 77(10):105901.
13. Coulier W, Sapsis TP (2015) Unsteady evolution of localized unidirectional deep-water wave groups. *Physical Review E* 91(6):063204.
14. Farhat M, Sapsis TP (2017) Reduced-order prediction of rogue waves in two-dimensional deep-water waves. *Journal of Computational Physics* 340:418–434.
15. Onorato M, Osborne AR, Serio M, Bertone S (2001) Freak waves in random oceanic sea states. *Physical Review Letters* 86(25):5831–5834.
16. Deniers G, Grafe T, Vanden-Eijnden E (2018) Rogue waves and large deviations in deep sea. *Proceedings of the National Academy of Sciences* 115(5):855–860.
17. Sergeeva A, Pelinovsky E, Talipova T (2011) Nonlinear random wave field in shallow water: variable Korteweg-de Vries framework. *Natural Hazards and Earth System Sciences* 11(2):329–330.
18. Trulsen K, Zeng H, Gramstad O (2012) Laboratory evidence of freak waves provoked by non-uniform bathymetry. *Physics of Fluids* 24(9):097101.
19. Viotti C, Dias F (2014) Extreme waves induced by strong depth transitions: Fully nonlinear results. *Physics of Fluids* 26(5):051705.
20. Bollt E, Speer K, Moore MNJ (2018) Anomalous wave statistics induced by abrupt depth change. *arXiv preprint arXiv:1808.07958*.
21. Johnson RS (1997) *A modern introduction to the mathematical theory of water waves*. (Cambridge University press) Vol. 19.
22. Abramov R, Kováčik G, Majda AJ (2003) Hamiltonian structure and statistically relevant conserved quantities for the truncated Burgers-Hopf equation. *Communications on Pure and Applied Mathematics: A Journal Issued by the Courant Institute of Mathematical Sciences* 56(16):1681–1680.
23. Majda AJ, Wang X (2006) *Nonlinear dynamics and statistical theories for basic geophysical flows*. (Cambridge University Press).
24. Bajars J, Frank J, Leimkuhler B (2013) Weakly coupled heat bath models for Gibbs-like invariant states in nonlinear wave equations. *Nonlinearity* 26(7):1945–1973.
25. McLachlan R (1993) Symplectic integration of hamiltonian wave equations. *Numerische Mathematik* 66(1):465–492.